

RESEARCH

Open Access



Can white matter lesion burden predict involvement of normal appearing thalami in multiple sclerosis? Study using 3D FLAIR and DTI

Mohamed D. Homos

Abstract

Background: Multiple sclerosis is a chronic demyelinating disease that affects the white and grey matter. The thalamus is responsible for many neurological functions, and it is liable to damage in multiple sclerosis in the absence of MRI-detectable thalamic lesions. Standardized imaging protocol for multiple sclerosis includes 3D FLAIR sequence that is highly sensitive in detecting white matter lesions. Owing to the thalamic functional importance, we aim in this study to show to what extent the standardized imaging protocol (3D FLAIR) can predict microscopic damage of normal appearing thalami, depending on DTI metrics (ADC and FA) as indicators of the microscopic damage.

Results: We examined 42 multiple sclerosis patients, 16 males and 26 females, with mean age 29 ± 6 years using 3D FLAIR sequence to delineate the white matter lesions and calculate their total areas and using DTI to calculate the average ADC and FA values of the thalami. Spearman's correlation coefficient (r) was used to correlate between the white matter lesion burden and the thalamic diffusivity (ADC and FA).

Moderate correlation was found between average ADC values of the thalami and the total white matter lesion areas ($r = 0.5, p = 0.03$).

Very weak correlation was found between average FA values of the thalami and the total white matter lesion areas ($r = -0.1, p = 0.6$).

Conclusion: White matter lesion burden detected using the highly sensitive 3D FLAIR sequence does not always correlate with the microstructural damage in normal appearing thalami. DTI needs to be added to the examination protocol if damage of normal appearing thalami is of concern.

Keywords: White matter lesion burden, Multiple sclerosis, DTI, 3D FLAIR

Background

Multiple sclerosis (MS) is a chronic autoimmune demyelinating disease of the central nervous system (CNS). Pathologically, it shows areas of focal inflammation, edema, glial reaction, and scarring. It appears on conventional magnetic resonance imaging (MRI) as multifocal demyelinating plaques throughout the CNS [1, 2]. The thalamus, as a relay organ, is involved in motor,

sensory, integrative functions as well as other functions such as sleep and memory. Pathologically, the thalamus is vulnerable to early involvement in MS [3–5] and its microscopic damage can occur before detecting thalamic lesions by conventional MRI [6, 7]. Such microscopic damage and the microstructural integrity of the tissues can be assessed using diffusion tensor imaging (DTI) [8] which is not included in the standardized imaging protocol for MS. The standardized protocol for baseline and follow-up MRI examinations for patients with suspected or clinically definite multiple sclerosis include T2, 2D, or

Correspondence: homosdr@gmail.com
Radiology Department, Kasr El Aini Hospital, Cairo University, Cairo, Egypt

3D fluid attenuation inversion recovery (FLAIR) as well as pre and post contrast T1 images [9]. FLAIR sequence is superior to T2WI for detection of MS plaques [10] and 3D FLAIR has increased lesional visibility compared to 2D FLAIR [11]. This study aims to disclose the relation between the white matter lesion (WML) burden detected by 3D FLAIR and diffusivity of normal appearing thalami detected by DTI and to what extent we can depend on 3D FLAIR as indicator of microscopic damage of normal appearing thalami.

Methods

Forty-two patients (16 males and 26 females, mean age 29 ± 6 years) with established diagnosis of MS were included in this retrospective study. These patients were referred from the neurology department in our institution to undergo MRI examination from Oct 2017 till Sep 2019. All the included patients are chronic MS patients who were previously diagnosed based on clinical, laboratory, electrophysiological, and previous MR studies. Patients in a state of clinical relapse or under corticosteroid therapy within 1 month of the study were excluded, in addition to exclusion of patients with contraindication to MRI examination (e.g. cerebral aneurysm clips and cardiac pacemakers) and claustrophobia. Patients who found to have any MRI-detectable lesions in the thalami (including lacunar infarcts and very small lesions) were also excluded from the study. The study was approved by the institutional ethics committee. All participants gave informed written consent.

Image acquisition

MR study was conducted using 1.5 Tesla machine (Achieva, Philips Medical systems, Best, The Netherlands) using 16channel SENSE head coil.

Imaging protocol includes T1-weighted images: repetition time (TR) 488 ms, echo time (TE) 15 ms, field of view (FOV) 230 mm, 18 sections with slice thickness 6 mm, and matrix 208×134 . T2-weighted images: repetition time (TR) 1000 ms, echo time (TE) 100 ms, field of view (FOV) 230 mm, 18 sections with slice thickness 6 mm, and matrix 192×156 . Post contrast T1-weighted imaging was done 4–5 min after IV administration of gadopentetate dimeglumine 0.1 mmol/kg. 3D FLAIR sequence: repetition time (TR) 4800 ms, echo time (TE) 307 ms, inversion time (TI) 1660 ms, field of view (FOV) 250 mm, 128 sections with slice thickness 1.2 mm, matrix 228×227 , and scan time 5 min. Diffusion-weighted imaging using singleshot pulsed gradientecho echoplanar sequence with diffusion encoding gradients in 15 noncollinear directions with $b = 0$ and $b = 800$ s/mm²: TR 8000 ms, TE 67 ms, 60 contiguous 2-mmthick axial sections, FOV 224 mm, matrix 112×128 , and number of signal averages 2.

Image analysis

The images were analysed using Philips extended work station (EWS) View Forum 2.6.

First, 3D FLAIR images were reviewed to confirm absence of abnormal MR signal within the thalami.

Every section of the FLAIR sequence was inspected to detect any high MR signal lesions within the white matter. Purely cortical lesions were not included in this study as special MR techniques, such as double inversion recovery images, are needed to visualize these lesions [12]. The margins of every lesion were manually traced using a computer mouse to completely surround the lesion without including adjacent normal white matter, grey matter, or CSF. Magnification of images was done

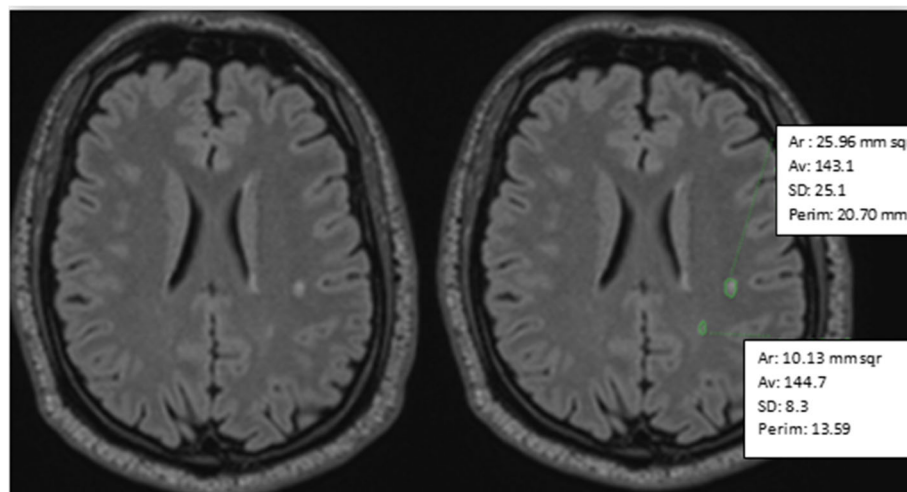


Fig. 1 Axial 3D FLAIR section showing two right cerebral demyelinating lesions (left). Manual tracing of the lesions with automatic calculation of their areas (right)

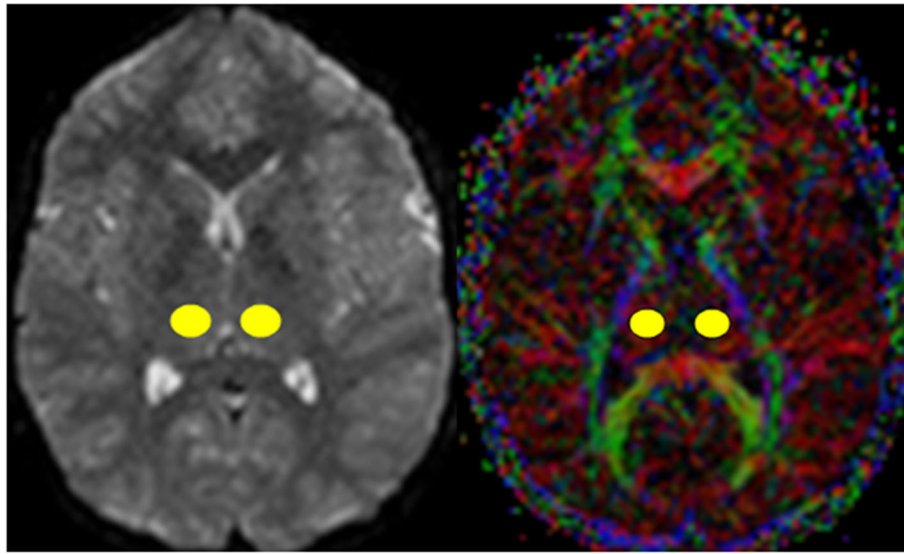


Fig. 2 Axial b₀ image (left) and FA map (right) showing ROI placed within both thalami to calculate ADC and FA values

to magnify small lesions in order to be able to trace their margins easily and accurately. After tracing, the area of the lesion can then be automatically calculated (Fig. 1). This was repeated in all the sections covering the entire brain. The sum of the measured areas was calculated to obtain the total area of lesions in all brain sections of the patient (as indicator of whole brain WML burden).

Automatic reconstruction of b₀ images, apparent diffusion coefficient (ADC), and fractional anisotropy (FA) maps from the echoplanar diffusion images was done. b₀ images show better anatomical details than ADC and FA maps, so allowing accurate placement of the region of interest (ROI). In the b₀ images, ROI was placed within the right and left thalami in three consecutive sections (ROI = 20 voxels). ROIs were placed within the widest parts of the thalami to ensure pure sampling of thalamic tissues (Fig. 2). Once a ROI placed within a b₀ image, an identical ROI will appear in the corresponding location in the ADC and FA maps. For each patient, average ADC and FA from the values of the three contiguous sections was calculated.

The radiological evaluation and post processing were done by an experienced radiologist, M.H. (more than 10 years' experience). Intra-observer agreement $\kappa = 0.56$

Statistical analysis

Continuous variables were presented as mean \pm SD. Categorical data were expressed as absolute frequencies and percentages. MannWhitney *U* test was used to test statistical significance. Spearman's correlation coefficient (*r*) was used to correlate between continuous variables where *r* ranges from -1 to 1 , positive values indicate linear positive correlation, and negative values indicate

linear negative correlation. When *r* is closer to 1 or -1 , the linear correlation is stronger.

The strength of the correlation is either very weak ($r = 0.00-0.19$), weak ($r = 0.2-0.39$), moderate ($r = 0.4-0.59$), strong ($r = 0.6-0.79$), or very strong ($r = 0.8-1.0$). *p* value < 0.05 was considered statistically significant. Statistical Package for the Social Sciences software (SPSS for Windows, version 15.0, SPSSInc. Chicago, IL) was used for statistical analysis.

Results

The MS plaques of the study group were detected in various white matter regions (Figs. 3, 4, 5, and 6). The periventricular and subcortical locations were the most common while the juxtacortical location is the least common. The distribution of WMLs in the study group is shown in Table 1.

Burden of WMLs in the study group

The sum of WML areas of patients included in this study ranged from 1.77 to 36.55 cm² with average 18.3 \pm 11cm². The burden of WMLs in the different white matter locations is shown in Table 1.

Table 1 The distribution of WMLs in the study group

Location	Number of patients (%)	WMLs' area in cm ² (%)
Periventricular	42 (100%)	11.3 (62%)
Subcortical	42 (100%)	3.8 (21%)
Juxtacortical	32 (76%)	1.3 (7%)
Posterior fossa	35 (83%)	1.8 (10%)

WMLs white matter lesions

Table 2 ADC and FA of the thalami in the subgroups according to the location of the lesions

Subgroup based on location	Average thalamic ADC ($\times 10^{-3} \text{ mm}^2/\text{s}$)	Average thalamic FA
Periventricular (N = 42)	0.771	0.45
Subcortical (N = 42)	0.771	0.45
Juxtacortical (N = 32)	0.753	0.47
Posterior fossa (N = 35)	0.766	0.44

Average ADC and FA of the thalami in the study group

Average ADC of the right thalami was $0.771 \pm 0.03 \times 10^{-3} \text{ mm}^2/\text{s}$, of the left thalami was $0.770 \pm 0.05 \times 10^{-3} \text{ mm}^2/\text{s}$, and of both right and left thalami was $0.771 \pm 0.026 \times 10^{-3} \text{ mm}^2/\text{s}$.

Average FA of the right thalami was 0.457 ± 0.06 , of the left thalami was 0.443 ± 0.06 , and of both right and left thalami was 0.45 ± 0.05 .

Correlation between thalamic ADC and WML area

Moderate correlation was found between average ADC values of the right thalami and total WML areas ($r = 0.4$, $p = 0.04$), while weak correlation was demonstrated between the average ADC values of the left thalami and the total WML areas ($r = 0.3$, $p = 0.03$). Correlation between average ADC values of the thalami and the total WML areas shows moderate correlation ($r = 0.5$, $p = 0.03$).

Correlation between thalamic FA and WML area

Very weak correlation was found between average FA values of the right thalami and the total WML areas ($r = 0.14$, $p = 0.5$), between average FA values of the left thalami and the total WML areas ($r = -0.3$, $p = 0.13$), as well as between average FA values of the thalami and the total WML areas ($r = -0.1$, $p = 0.6$).

Correlation between the thalamic DTI metrics and WML load in different locations

ADC and FA of the thalami in the subgroups according to the location of the lesions are shown in Table 2.

Periventricular and subcortical lesions were seen in the whole study group and showed the highest WML load and the highest thalamic ADC values while the juxtacortical lesions had the lowest WML load and the lowest ADC values, ($r = 0.9$, $p = 0.04$).

Very weak correlation was found between the WML burden in different locations and FA values ($r = 0.3$, $p = 0.6$).

Discussion

In this study, we found that the burden of WMLs detected by 3D FLAIR sequence has a moderate degree of influence on the diffusivity of water molecules (ADC values) within the normal appearing thalami ($p < 0.05$). This is in accordance with a study by Cappellani and colleagues [13] that showed an association between T2 lesion load and diffusivity within the subcortical deep grey matter (thalami, caudate and hippocampi) ($p < 0.05$). However, in our study, 3D FLAIR was used which has higher sensitivity for WML detection compared to the T2 images used by Cappellani and colleagues. Also, the effect of WMLs load on the thalami was demonstrated by another study by Henry and colleagues [4] that showed significant correlation between the volume of the WMLs in the corticothalamic pathway and the thalamic volume ($p < 0.001$). This relation could be explained by the microstructural damage occurring in the thalami secondary to retrograde degeneration of the white matter fibres that pass within the white matter MS plaques [13, 14]. Such damage causes widening of the extracellular CSF spaces within the thalami and subsequently increases the

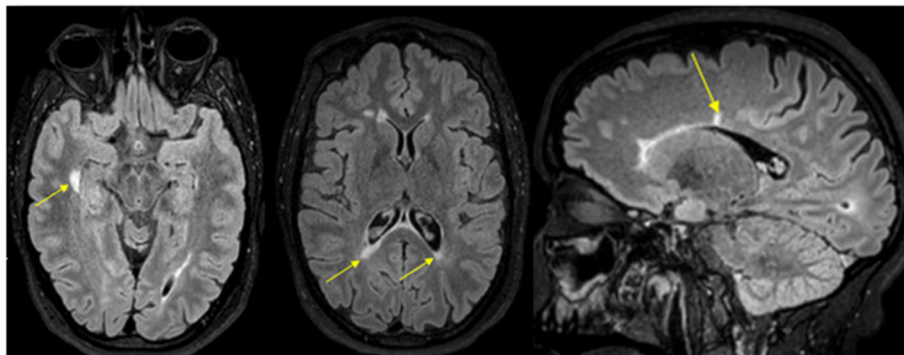


Fig. 3 Axial and sagittal 3D FLAIR sections showing periventricular white matter lesions abutting the lateral ventricles with no white matter in between

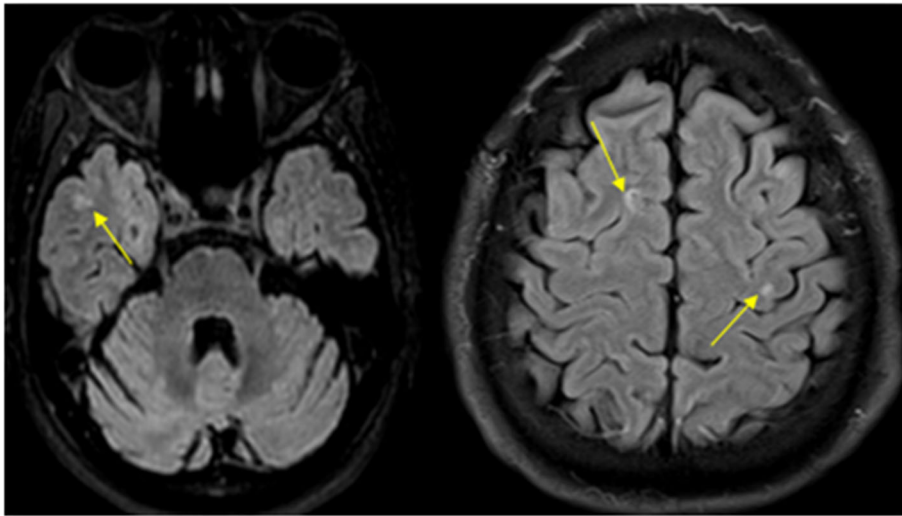


Fig. 4 Axial 3D FLAIR sections showing juxtacortical white matter lesions abutting the cortex with no white matter in between

diffusivity of the water molecules which can be detected using ADC values. However, the degree of correlation between the WML burden and thalamic diffusivity was found to be a moderate, and not strong, correlation. This can point to the presence of other factors affecting the diffusivity of the thalami besides the retrograde degeneration. It has been stated that primary grey matter injury in MS can occur secondary to deposition of iron, inflammatory processes, in addition to demyelination and neurotoxicity [15]. Also, the thalamic diffusivity can be affected by the widespread microstructural changes occurring in the

normal appearing white matter in MS patients that are probably related to demyelination, axonal degeneration, and secondary adaptive changes of already existing brain MS lesions [16] that is in turn reflected upon the thalamic diffusivity.

Anisotropy is a measure of fibre integrity and directionality where water molecules move more easily parallel to white matter tracts than perpendicular to them [17]. In our study, the WML burden was found to have almost no influence on anisotropy within the thalami ($p > 0.05$) in agreement with a previous study done on

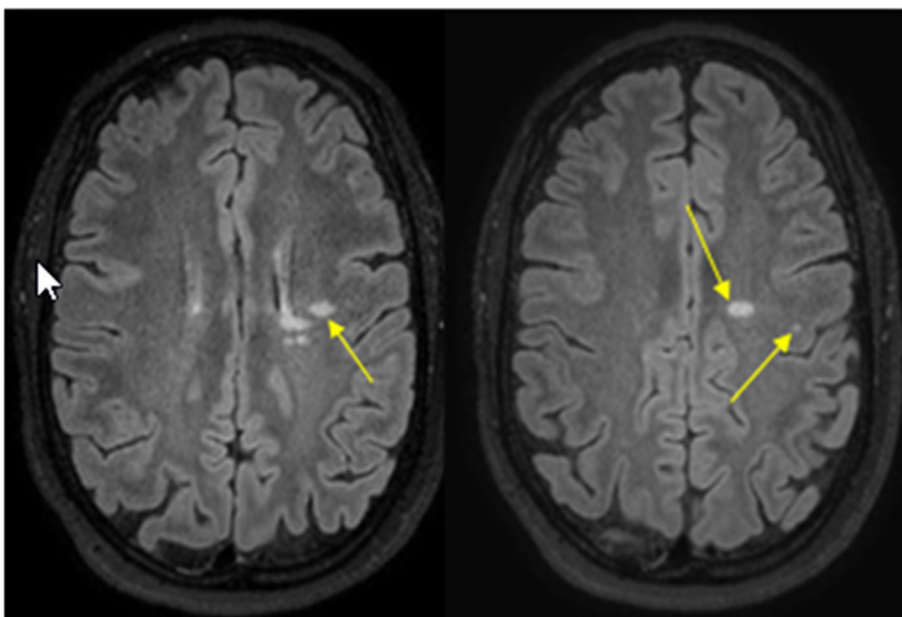


Fig. 5 Axial 3D FLAIR sections showing subcortical white matter lesions separated from the cortex by white matter

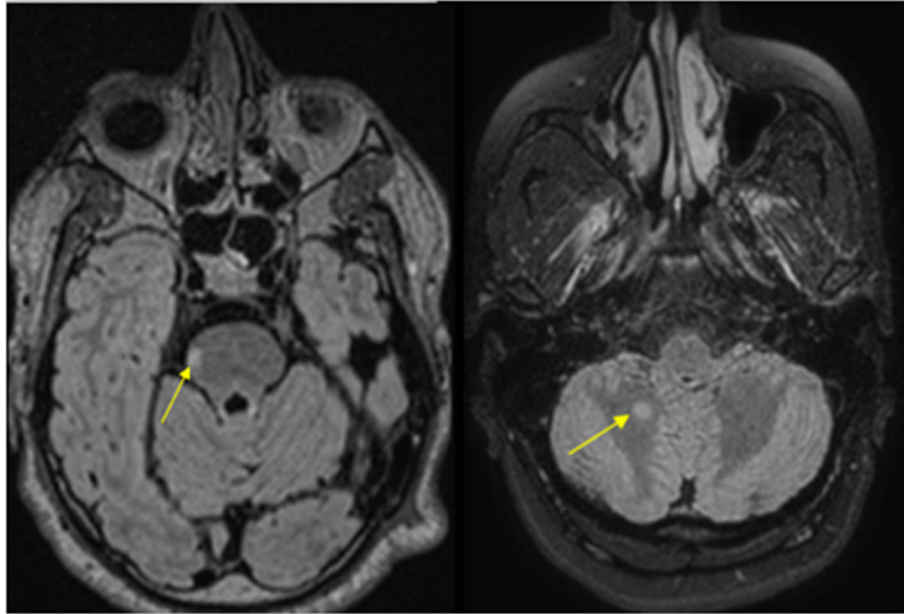


Fig. 6 Axial 3D FLAIR sections showing infratentorial white matter lesions

the subcortical grey matter [13] that showed no association between FA of the subcortical deep grey matter and T2 lesions load ($p > 0.05$). This can be explained by the non-uniform effect of the pathological changes in MS on anisotropy. Demyelination, axonal loss, and inflammatory cells' accumulation reduce anisotropy while reduction of the dendritic arborization will increase coherence and subsequently increases anisotropy [17]. We concluded that WML burden detected using the highly sensitive 3D FLAIR sequence does not always correlate with the microstructural damage in normal appearing thalami. So, the standardized protocol of MR examination of MS patients is not sufficient if the pathological damage in normal appearing thalami need to be assessed. DTI needs to be added to the examination protocol in such cases to assess thalamic damage.

This study may have a limitation of using manual method, rather than the automatic segmentation method, to delineate WMLs. The used manual method is more time-consuming and is liable to interobserver variability. However, it was preferred to be used in this study, as WMLs imaged by the standardized protocol are only visually assessed in clinical practice. Also, investigating all the MS subtypes as one group, without dividing them into subgroups, can be a limitation of this study.

Future studies can be conducted to disclose combined effect WML burden and diffusivity of normal appearing white matter on the thalami.

Abbreviations

ADC: Apparent diffusion coefficient; CNS: Central nervous system; CSF: Cerebrospinal fluid; DTI: Diffusion tensor imaging; FA: Fraction

anisotropy; FLAIR: Fluid attenuation inversion recovery; MRI: Magnetic resonance imaging; MS: Multiple sclerosis; ROI: Region of interest; WML: White matter lesion

Acknowledgements

Not applicable.

Author's contributions

MDH has collected, interpreted, and analysed the data and prepared the article. The author read and approved the final manuscript.

Funding

Not applicable

Availability of data and materials

The datasets generated and/or analysed during this study are available from the corresponding author on reasonable request.

Ethics approval and consent to participate

This study was approved by Kasr Alaini Cairo University hospital research ethics committee. Number: not available. Written informed consents were signed by the patients.

Consent for publication

All patients included in this research gave written informed consent to publish the data contained within this study.

Competing interests

The author declares that he has no competing interests.

Received: 22 July 2020 Accepted: 1 January 2021

Published online: 13 January 2021

References

1. Reich DS, Lucchinetti CF, Calabresi PA (2018) Multiple sclerosis. *N Engl J Med* 378:169–180. <https://doi.org/10.1056/NEJMra1401483>
2. Brownlee WJ, Hardy TA, Fazekas F, Miller DH (2017) Diagnosis of multiple sclerosis: progress and challenges. *Lancet Lond Engl* 389:1336–1346. [https://doi.org/10.1016/S0140-6736\(16\)30959-X](https://doi.org/10.1016/S0140-6736(16)30959-X)
3. Henry RG, Shieh M, Okuda DT, Evangelista A, Gorno-Tempini ML, Pelletier D (2008) Regional grey matter atrophy in clinically isolated syndromes at

- presentation. *J Neurol Neurosurg Psychiatry* 79:1236–1244. <https://doi.org/10.1136/jnnp.2007.134825>
4. Henry RG, Shieh M, Amirbekian B, Chung S, Okuda DT, Pelletier D (2009) Connecting white matter injury and thalamic atrophy in clinically isolated syndromes. *J Neurol Sci* 282:61–66. <https://doi.org/10.1016/j.jns.2009.02.379>
 5. Ramasamy DP, Benedict RHB, Cox JL, Fritz D, Abdelrahman N, Hussein S et al (2009) Extent of cerebellum, subcortical and cortical atrophy in patients with MS: A case-control study. *J Neurol Sci* 282:47–54. <https://doi.org/10.1016/j.jns.2008.12.034>
 6. Cifelli A, Arridge M, Jezzard P, Esiri MM, Palace J, Matthews PM (2002) Thalamic neurodegeneration in multiple sclerosis. *Ann Neurol* 52:650–653. <https://doi.org/10.1002/ana.10326>
 7. Kutzelnigg A, Lassmann H (2005) Cortical lesions and brain atrophy in MS. *J Neurol Sci* 233:55–59. <https://doi.org/10.1016/j.jns.2005.03.027>
 8. Tovar-Moll F, Evangelou IE, Chiu AW, Richert ND, Ostuni JL, Ohayon JM et al (2009) Thalamic involvement and its impact on clinical disability in patients with multiple sclerosis: a diffusion tensor imaging study at 3 T. *AJNR Am J Neuroradiol* 30:1380–1386. <https://doi.org/10.3174/ajnr.A1564>
 9. Rovira A, Wattjes MP, Tintoré M, Tur C, Yousry TA, Sormani MP et al (2015) Evidence-based guidelines: MAGNIMS consensus guidelines on the use of MRI in multiple sclerosis-clinical implementation in the diagnostic process. *Nat Rev Neurol* 11:471–482. <https://doi.org/10.1038/nrneurol.2015.106>
 10. Gabr RE, Pednekar AS, Govindarajan KA, Sun X, Riascos RF, Ramírez MG et al (2017) Patient-specific 3D FLAIR for enhanced visualization of brain white matter lesions in multiple sclerosis. *J Magn Reson Imaging* 46:557–564. <https://doi.org/10.1002/jmri.25557>
 11. Polak P, Magnano C, Zivadinov R, Poloni G (2012) 3D FLAIRE: 3D fluid attenuated inversion recovery for enhanced detection of lesions in multiple sclerosis. *Magn Reson Med* 68:874–881. <https://doi.org/10.1002/mrm.23289>
 12. Thompson AJ, Banwell BL, Barkhof F, Carroll WM, Coetzee T, Comi G et al (2018) Diagnosis of multiple sclerosis: 2017 revisions of the McDonald criteria. *Lancet Neurol* 17:162–173. [https://doi.org/10.1016/S1474-4422\(17\)30470-2](https://doi.org/10.1016/S1474-4422(17)30470-2)
 13. Cappellani R, Bergsland N, Weinstock-Guttman B, Kennedy C, Carl E, Ramasamy DP et al (2014) Subcortical deep gray matter pathology in patients with multiple sclerosis is associated with white matter lesion burden and atrophy but not with cortical atrophy: a diffusion tensor MRI study. *Am J Neuroradiol* 35:912–919. <https://doi.org/10.3174/ajnr.A3788>
 14. Ceccarelli A, Rocca MA, Falini A, Tortorella P, Pagani E, Rodegher M et al (2007) Normal-appearing white and grey matter damage in MS. A volumetric and diffusion tensor MRI study at 3.0 Tesla. *J Neurol* 254:513–518. <https://doi.org/10.1007/s00415-006-0408-4>
 15. Fabiano AJ, Sharma J, Weinstock-Guttman B, Munschauer FE, Benedict RH, Zivadinov R et al (2003) Thalamic involvement in multiple sclerosis: a diffusion-weighted magnetic resonance imaging study. *J Neuroimaging Off J Am Soc Neuroimaging* 13:307–314
 16. Kim S-H, Kwak K, Hyun J-W, Joung A, Lee SH, Choi Y-H et al (2017) Diffusion tensor imaging of normal-appearing white matter in patients with neuromyelitis optica spectrum disorder and multiple sclerosis. *Eur J Neurol* 24:966–973. <https://doi.org/10.1111/ene.13321>
 17. Inglese M, Bester M (2010) Diffusion imaging in multiple sclerosis: research and clinical implications. *NMR Biomed* 23:865–872. <https://doi.org/10.1002/nbm.1515>

Publisher's Note

Springer Nature remains neutral with regard to jurisdictional claims in published maps and institutional affiliations.

Submit your manuscript to a SpringerOpen[®] journal and benefit from:

- Convenient online submission
- Rigorous peer review
- Open access: articles freely available online
- High visibility within the field
- Retaining the copyright to your article

Submit your next manuscript at ► [springeropen.com](https://www.springeropen.com)